Feedback Control of Oxygen Uptake During Robot-Assisted Gait

Andrew Pennycott, Kenneth J. Hunt, Sylvie Coupaud, David B. Allan, and Tanja H. Kakebeeke

***Abstract*—Body-weight-supported robot-assisted devices can be used to promote gait rehabilitation and as exercise tools for neurologically impaired persons such as stroke and spinal-cord-injured patients. Here, we propose a novel feedback-control structure for real-time control of oxygen uptake during robot-assisted gait, in which we use the following methods. 1) A feedback-control structure is proposed, consisting of a dynamic controller operating on target and actual levels of oxygen uptake in order to set a target work rate. Target work rate is achieved by an inner volitional feedback loop which relies on the subject's exercise input. 2) The dynamic oxygen-uptake controller is based on an empirically derived model of the oxygen-uptake dynamics and is synthesized by pole placement. 3) The resulting control system is tested during the robot-assisted treadmill ambulation of five able-bodied subjects. A single linear controller was designed based on identification data from tests with one subject and used for closed-loop control tests with all five subjects. In all cases, the actual oxygen-uptake response closely followed the ideal response as specified by the feedback design parameters. The control of oxygen uptake during body-weight-supported robot-assisted ambulation is feasible in the able-bodied population; the robustness of the system is demonstrated within the class of subjects tested. Further testing is required to validate the approach with neurologically impaired subjects.**

***Index Terms*—Feedback control, rehabilitation engineering, robot-assisted gait, spinal-cord injury, system identification.**

I. Introduction

ROBOT-ASSISTED body-weight-supported treadmill training (rBWSTT) is normally used in a rehabilitation setting for the gait training of subjects with neurological deficits such as stroke and incomplete spinal-cord injury. The main advantages of the robotic system over conventional therapist-assisted walking include the repeatability of the gait and the fact that it is less labor intensive for the physiotherapists responsible for its implementation [1]. Research has demonstrated that rBWSTT can elicit improvements in treadmill walking [2], [3]. Moreover, due to the significant cardiovascular response which can be observed during ambulation [4]–[6], the technology has additional potential as an exercise tool for people with neurological impairment. This is important since the spinal-cord-injured population suffers from a number of secondary health conditions [7] whose severity may be reduced by effective exercise [8], [9]. rBWSTT may provide an additional training platform to subjects for whom other options such as functional electrical stimulation may not be feasible due to residual sensation; moreover, robotic treadmill training may be more effective than arm-based exercise since it employs a larger muscle mass and can therefore elicit a greater cardiovascular response.

A measure of a subject's volitional input to the exercise is important since active encouragement may be required. The work done by a subject will tend to be smaller in robot-assisted walking than in manual therapist-assisted ambulation due to the mechanical assistance available in the former case [2], [4]. Initial investigation into biofeedback application was undertaken by Lünenburger *et al.* where a weighted combination of forces was used to determine the relative effort of an exercising subject [10], [11]. Our group has previously presented the use of a feedback-controlled system incorporating an estimate of active work rate and volitional input in order to produce work-rate levels in close agreement with predetermined desired levels [12]–[14].

Expanding on the ability to control mechanical variables during rBWSTT, a natural progression is to examine the feasibility of regulating the corresponding physiological variables. Heart rate is available for measurement and control but is influenced by several factors including emotional state, pain, and hydration level [15], making it difficult to use in real-time control. Therefore, the natural choice of control variables is the rate of oxygen uptake $\dot{V}_{O_2}$. The control of $\dot{V}_{O_2}$ would allow the exercise to be performed at a predetermined relative intensity (i.e., percentage of maximal capacity) as often recommended [16]. Regulating oxygen uptake to desired levels would also be useful during exercise testing where a specific profile of intensity is required. Successful feedback control of oxygen uptake may be found in the areas of treadmill running [13] and functional electrical stimulation cycling [17].

The aim of this paper is to investigate the feasibility of real-time feedback control of oxygen uptake during robot-assisted gait. We propose a novel feedback system for the automatic control of oxygen uptake based on an empirical model of the underlying dynamic system determined from system-identification sessions. We then present results of an experimental feasibility study where the proposed feedback system was tested during robot-assisted treadmill ambulation of five able-bodied subjects.

II. Methods

A. Procedures

The individual steps carried out in this study were system identification, offline model estimation and validation, calcula-

Manuscript received November 05, 2007; revised September 16, 2008. First published April 28, 2009; current version published December 23, 2009. Recommended by Associate Editor J. Raisch.

A. Pennycott, K. J. Hunt, and S. Coupaud are with the Centre for Rehabilitation Engineering, Department of Mechanical Engineering, University of Glasgow, Glasgow G12 8QQ, U.K., and also with The Scottish Centre for Innovation in Spinal Cord Injury, Glasgow, G51 4FT, U.K.

D. B. Allan is with The Scottish Centre for Innovation in Spinal Cord Injury, Glasgow, G51 4FT, U.K., and also with the Queen Elizabeth National Spinal Injuries Unit, Southern General Hospital, Glasgow, G51 4TF, U.K.

T. H. Kakebeeke is with the Department of Medicine, University of Fribourg, Fribourg CH-1700, Switzerland.

Color versions of one or more of the figures in this paper are available online at http://ieeexplore.ieee.org.

Digital Object Identifier 10.1109/TCST.2008.2009465

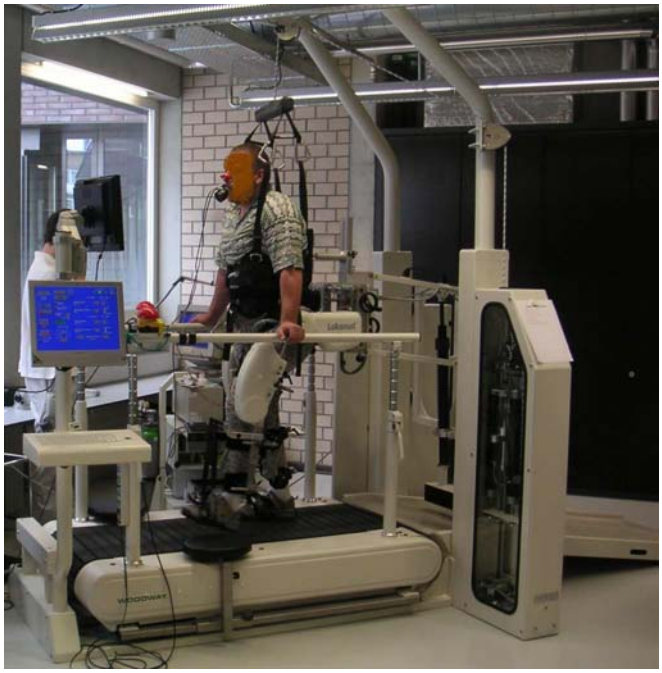

Fig. 1. Lokomat in operation with robotic orthoses, treadmill, weight-support mechanism, and breath-by-breath system shown.

tion of control system parameters, and real-time feedback-control tests. Five able-bodied subjects were used for the tests.

System-identification tests were used to determine empirical models relating the $\dot{V}_{O_2}$ response to the work rate. Following the estimation of the model parameters based on a least squares analysis of the collected data, the models were validated using a fit criterion.

Offline control design and analysis were carried out based on the empirical models, employing a pole-placement scheme. Experimental real-time feedback-control tests were then carried out in order to validate the proposed control method.

B. Apparatus and Data Processing

The research employed a driven-gait orthosis device (Lokomat, Hocoma AG, Switzerland) shown in Fig. 1, in combination with a treadmill (Woodway GmbH, Germany). The subject was fitted to robotically driven orthotic limbs via adjustable straps, and a portion of the body weight was supported via a harness using a specialized feedback-controlled lift device (Lokolift, Hocoma AG, Switzerland) [18].

Force and angular position measurements at the robotic joints were sampled at 5 Hz by means of custom-written software and interface equipment and were read into a laptop computer (Latitude D610, Dell, USA) using a data acquisition card (USB-6009, National Instruments, USA). Processing and calculation in real time were undertaken using a numerical computing package (MATLAB, Mathworks, USA).

Oxygen uptake was measured in real time using a breath-by-breath measuring system (MetaMax 3B, Cortex Biophysik GmbH, Germany). The system is comprised of a low dead-space mask, a gas analyzer to measure gas composition, and a turbine for the measurement of volume flow rate. Prior to each test, the volume transducer was calibrated by means of a 3-L syringe while the gas analyzer was calibrated via a two-point calibration with atmospheric air and a reference gas of known (certified) composition.

TABLE I
SUBJECT DETAILS. PHYSICAL CHARACTERISTICS OF THE SUBJECTS ARE NOTED ALONG WITH THE DEGREE OF BODY-WEIGHT SUPPORT PROVIDED

Subject	Age (yr)	Sex	Mass (kg)	BWS (kg)	Height (cm)
S_A	21	m	72	50	173
S_B	20	m	72	50	178
S_C	30	m	98	70	182
S_D	22	f	62	45	160
S_E	29	m	71	50	174

$\dot{V}_{O_2}$ data are not produced at regular intervals but at time instants corresponding to each breath. In order to give a constant sampling interval for real-time control, the breath-by-breath data were averaged over 20-s periods, this corresponding to the sampling frequency employed during system identification and real-time control. Although this introduces a delay, this is short compared with the timescales of the $\dot{V}_{O_2}$ dynamics. Such an averaging period results in approximately ten samples per rise time of the closed-loop system (specified as 200 s—see Section II-G) and is thus in accordance with heuristic-control system design rules [19].

C. Subjects

Five able-bodied subjects were selected for the tests; the subjects' details are displayed in Table I. Subjects were students of the University of Glasgow and were required to have no health problems. The subjects gave their informed written consent prior to the experimentation. The study was approved by the South Glasgow and Clyde Research Ethics Committee.

D. Plant Dynamics: Volitional Control of Work Rate

Our group has previously demonstrated the use of a work-rate estimate as part of a feedback-controlled system to regulate work rates to target values during robot-assisted gait, relying on volitional input from the subject as described in [14].

The essence of this estimation method is that the net rate of work done $\dot{W}_{\text{net}}$ is approximately constant, irrespective of the contribution of the exercising person to the gait. This arises because the actuators of the machine act so as to keep the gait in a constant trajectory. There are two distinct scenarios. In the first, denoted passive walking, the subject does not contribute to the work done required for propulsion, with the power to sustain walking being derived solely from the Lokomat itself. In the active case, some degree of work done is provided by the subject via volitional muscle forces $\dot{W}_S^A$ [20]. Denoting the powers from the Lokomat in the passive and active cases as $\dot{W}_L^P$ and $\dot{W}_L^A$, respectively, and using the fact that the net work rate is constant

$$\dot{W}_{\text{net}} = \dot{W}_L^P = \dot{W}_L^A + \dot{W}_S^A \tag{1}$$

and the active subject power is given by

$$\dot{W}_S^A = \dot{W}_L^P - \dot{W}_L^A. \tag{2}$$

$\dot{W}_L^A$ can be calculated online during a test. $\dot{W}_L^P$ is measured during a separate test where passive walking is performed, and

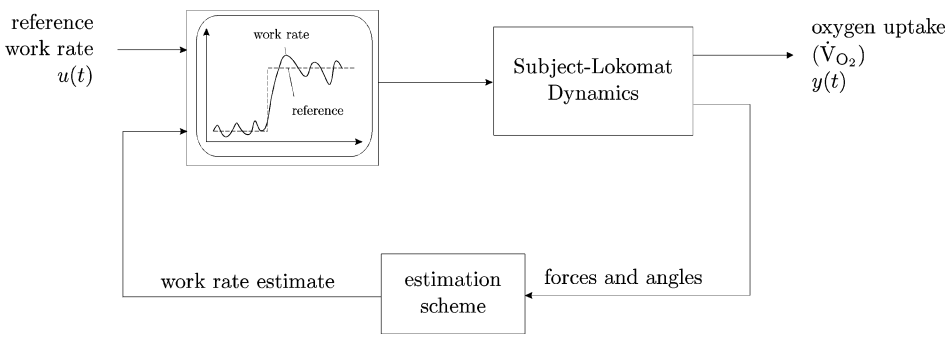

Fig. 2. Underlying dynamic system (plant). The outputs of the system are the work rate and oxygen-uptake rate $\dot{V}_{O_2}$, both of which respond to the reference work-rate input. The subject's volitional control efforts form an integral part of the plant.

a Fourier series approximation is calculated from these data that can be used to determine its value at each point in the gait cycle during an active walking test.

The subject uses this online estimate of work rate and compares it to a reference signal and adjusts his level of effort so that the reference (desired) work-rate level is produced. This is achieved by displaying the estimated and reference work rates to the subject on a flat-panel screen at the front of the treadmill (Fig. 1). The different work rates produced also give rise to variations in the $\dot{V}_{O_2}$ level. The resulting system for volitional work-rate control and oxygen-uptake forcing is shown in Fig. 2. For the purposes of oxygen-uptake control, the "plant" is considered to be the pathway from reference work rate $u(t)$ to oxygen uptake $y(t)$.

E. System Identification

Empirical models of the system in Fig. 2 were determined via separate system-identification tests where a $\dot{V}_{O_2}$ output was elicited using a reference-work-rate signal of pseudorandom binary sequence form. From the input–output data, an autoregressive with exogenous input (ARX) model was determined for each subject [21]. Writing in terms of the backward-shift operator q^{-1}, the plant model is given by

$$y(t) = \frac{q^{-k}B(q^{-1})}{A(q^{-1})}u(t) + \frac{1}{A(q^{-1})}d(t). \tag{3}$$

Here

$$A(q^{-1}) = 1 + a_1 q^{-1} + a_2 q^{-2} + \cdots + a_{n_a} q^{-n_a} \tag{4}$$
$$B(q^{-1}) = b_0 + b_1 q^{-1} + \cdots + b_{n_b} q^{-n_b}. \tag{5}$$

$u(t)$ and $y(t)$ are the work-rate reference and the $\dot{V}_{O_2}$ output, respectively, as shown in Fig. 2. The ARX model is also driven by the stochastic disturbance input $d(t)$.

The data set from each test was partitioned into two sections to give estimation and validation sets. The estimates of the plant polynomials A and B were obtained by least squares. In order to compare the various model structures produced during identification, the fit criterion of (6) was used

$$fit = 100\left[1 - \left(\frac{\sum_{t=1}^{N}(y(t) - \hat{y}(t))^2}{\sum_{t=1}^{N}(y(t) - \bar{y})^2}\right)^{0.5}\right]. \tag{6}$$

In this equation, $y(t)$ and $\hat{y}(t)$ are the measured and modeled $\dot{V}_{O_2}$ output, respectively, at time t and $\bar{y}$ is the mean of the measured output signal. Therefore, the fit criterion uses the N sampled data points to determine the percentage of the output variance that is accounted for by a given model.

Identification tests were carried out for each subject, and the best data set (in terms of fit) was selected from these to provide a discrete-time model for control synthesis. One controller based on this model was used throughout all real-time control testing, providing the opportunity to investigate the robustness of the closed-loop approach.

F. Proposed Feedback System For Control of $\dot{V}_{O_2}$

Fig. 3 shows the proposed control structure for the regulation of $\dot{V}_{O_2}$. In this novel setup, the volitional work-rate system of Fig. 2 assumes the role of the plant, while the $\dot{V}_{O_2}$ controller adjusts the level of reference work rate such that the $\dot{V}_{O_2}$ meets the reference oxygen uptake. The following sections address the design of the $\dot{V}_{O_2}$ controller.

G. Control Design by Pole Placement

The generic linear feedback structure of Fig. 4 was used here to represent the physical system of Fig. 3 for the purposes of controller synthesis and analysis. The control polynomials $R(q^{-1})$, $S(q^{-1})$, and $T(q^{-1})$ are calculated based on the closed-loop transfer function of this structure. The control output $u(t)$ was realized by (7), with the measurement of the output $y(t)$ being corrupted by the noise term $n(t)$ to give $y'(t)$

$$u(t) = \frac{1}{R}\left(Tr(t) - Sy'(t)\right). \tag{7}$$

With this arrangement, the overall closed-loop equation governing the response of the output to the various system inputs is given by

$$y(t) = \frac{q^{-k}BT}{AR + q^{-k}BS}r(t) + \frac{R}{AR + q^{-k}BS}d(t) - \frac{q^{-k}BS}{AR + q^{-k}BS}n(t). \tag{8}$$

In order to yield a desirable system behavior, the denominator common to each term of (8) was set to be the product of two

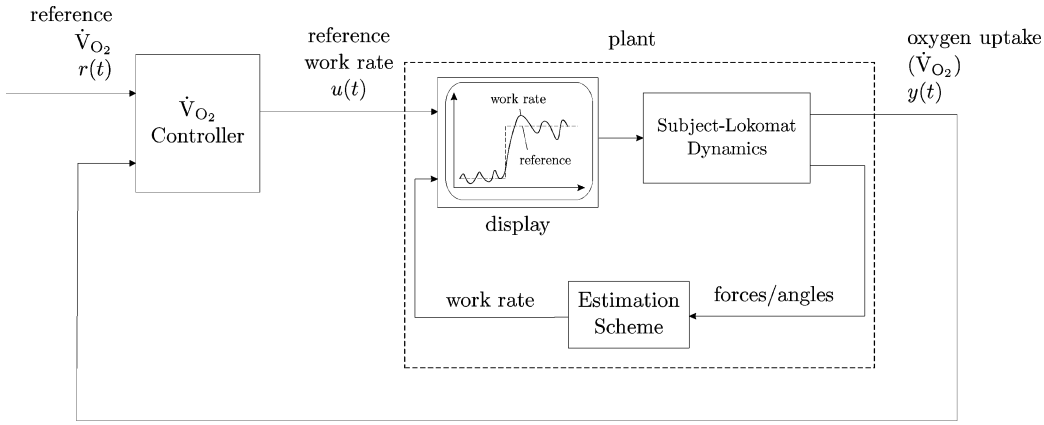

Fig. 3. Proposed feedback system for control of $\dot{V}_{O_2}$. The system output of the oxygen-uptake rate ($\dot{V}_{O_2}$) responds to a given reference work rate. A controller is developed which adjusts the level of reference work rate and thereby yields the desired $\dot{V}_{O_2}$.

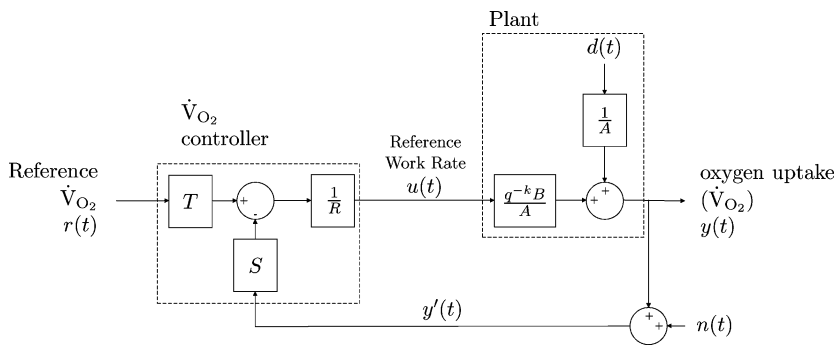

Fig. 4. Linear block diagram equivalent of the proposed feedback-control structure in Fig. 3. A and B are polynomials of the empirical plant model while R, S, and T are calculated from a pole-placement design scheme.

polynomials A_m and A_o, called the control and observer polynomials, respectively, [19]

$$AR + q^{-k}BS = A_o A_m. \tag{9}$$

Equation (9) was solved to give the control polynomials R and S. Integral action was incorporated by introducing the polynomial $(1 - q^{-1})$ as a factor of R.

T was made up of the observer polynomial A_o and a constant term λ; in this way, the response to the reference input $r(t)$ was governed by the control polynomial A_m but not by the observer polynomial A_o due to forced cancellation [19]

$$T = \lambda A_o. \tag{10}$$

With these relationships, the transfer function relating $r(t)$ and $y(t)$ is $q^{-k}\lambda B/A_m$. λ was set so as to give a unity steady-state gain as $\lambda = A_m(1)/B(1)$.

During the synthesis of the controller, the properties of the control and observer polynomials were specified in terms of rise times and damping factors of equivalent second-order continuous-time transfer functions[1]; equivalent polynomials in discrete time were determined numerically from the denominators of the resulting transfer functions. The control polynomial was specified to have a rise time of 200 s and a damping factor of 0.9, while the observer polynomial was assigned a rise time of 50 s and a damping factor of 0.9. The corresponding polynomials A_m and A_o which yield these specifications could then be calculated and (9) and (10) solved for R, S, and T.

H. Feedback-Control-Test Procedure

In order to validate the control approach experimentally, the closed-loop system was tested during the ambulation of five able-bodied subjects in the Lokomat. The control tests comprised of three phases, as shown in Fig. 5. The first of these was a rest phase where the subject stood in the Lokomat and the baseline $\dot{V}_{O_2}$ was measured. During the second phase, the subject was passively moved by the machine and did not attempt to contribute to the walking motion, allowing the parameters of the work-rate-estimation algorithm to be determined [14]. Toward the end of the passive phase, the controller was activated. However, since the reference $\dot{V}_{O_2}$ was, at this point, designed to reflect the $\dot{V}_{O_2}$ during the passive walking of that subject, the actual reference work rates, as generated by the controller, should be close to zero until the last phase. During the final active-control phase, the reference $\dot{V}_{O_2}$ alternated between two set levels in a square-wave function, a simple form of reference signal that demonstrates the dynamics of the closed-loop system following

[1]The polynomials were chosen to be second, rather than first, order so that the specified closed-loop response had a more general form, allowing system robustness with, e.g., different damping factors to be investigated.

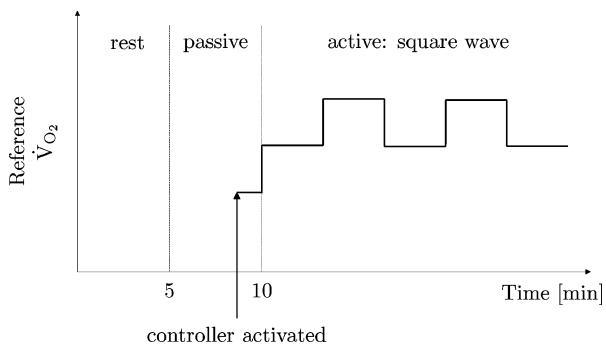

Fig. 5. Format of $\dot{V}_{O_2}$ reference signal for the feedback-control tests. Each test consisted of a rest phase, a passive phase, and an active phase, during which the reference $\dot{V}_{O_2}$ was varied as a square wave.

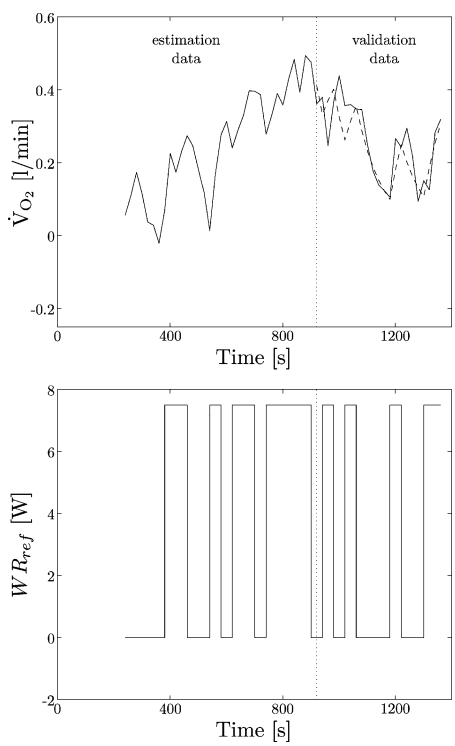

Fig. 6. Experimental identification test results of subject S_A. The oxygen-uptake-rate ($\dot{V}_{O_2}$) output is shown along with the work-rate input, with measured data being shown as solid lines. For the validation data, the simulated output of the arx111 model is included as a dashed line.

a change in reference input and also the ability of the controller to achieve a steady-state response with zero error.

III. Results

A. Identification-Test Data

The identification test with subject S_A yielded the highest value of fit among all the subjects; data from this test are shown in Fig. 6, with averaged measured data being shown as solid lines. In addition, for the validation data, the output, as simulated by a first-order model (arx111) calculated from the estimation data set, is included as a dashed line in order to demonstrate the accuracy achieved by the modeling.

TABLE II
Values of fit (in Percent) Achieved Using Different Model Orders for Subject S_A. The Model Structures Are Indexed According to the Number of Coefficients of A and B—which Are n_a and n_b+1, Respectively—and the Value of the Delay k. Therefore, arxABC Is an ARX Model With$(n_a, n_b+1, k) = (A, B, C)$

model	fit
arx111	42.5
arx112	33.2
arx113	11.6
arx114	6.1
arx211	44.2
arx212	40.3
arx213	11.8
arx214	3.8
arx311	45.1
arx312	45.8
arx313	11.7
arx314	-
arx411	52.5
arx412	46.8
arx413	7.6
arx414	-

B. Model Validation

The validation data of subject S_A are shown in Table II, displaying the values of fit achieved for the different model structures. Since it is normally considered advantageous to use a low order of the model for control design, the arx111 model structure was selected for control synthesis for its low-order and relatively high fit. This model has a rise time of approximately 200 s and has the following:

$$y(t) = \frac{q^{-1}(0.01127)}{(1-0.8602q^{-1})}u(t) + \frac{1}{(1-0.8602q^{-1})}d(t). \quad (11)$$

One controller was synthesized based on this model and subsequently used in all real-time feedback-control testing with all subjects, allowing the robustness of the proposed control approach to be investigated.

C. Computed Controller Polynomials

With the design specifications as in Section II-G, the computed polynomials R, S, and T were found to be

$$R(q^{-1}) = 1.00 - 1.46q^{-1} + 0.55q^{-2} - 0.09q^{-3} \quad (12)$$
$$S(q^{-1}) = 15.62 - 12.69q^{-1} \quad (13)$$
$$T(q^{-1}) = 5.77 - 3.55q^{-1} + 0.72q^{-2}. \quad (14)$$

These control polynomials, nominal for subject S_A, were used in all of the real-time feedback-control tests for all subjects. The vector margin of the closed-loop system, defined as the minimum distance from the Nyquist plot to the critical point $(-1, 0)$, was computed to be 0.84 for S_A, thus indicating good stability margins.

D. Experimental Control Test Results

The results of the control tests of the five subjects are shown in Fig. 7, displaying the measured $\dot{V}_{O_2}$ levels as solid lines, reference values as dashed lines, and the ideal responses as dotted

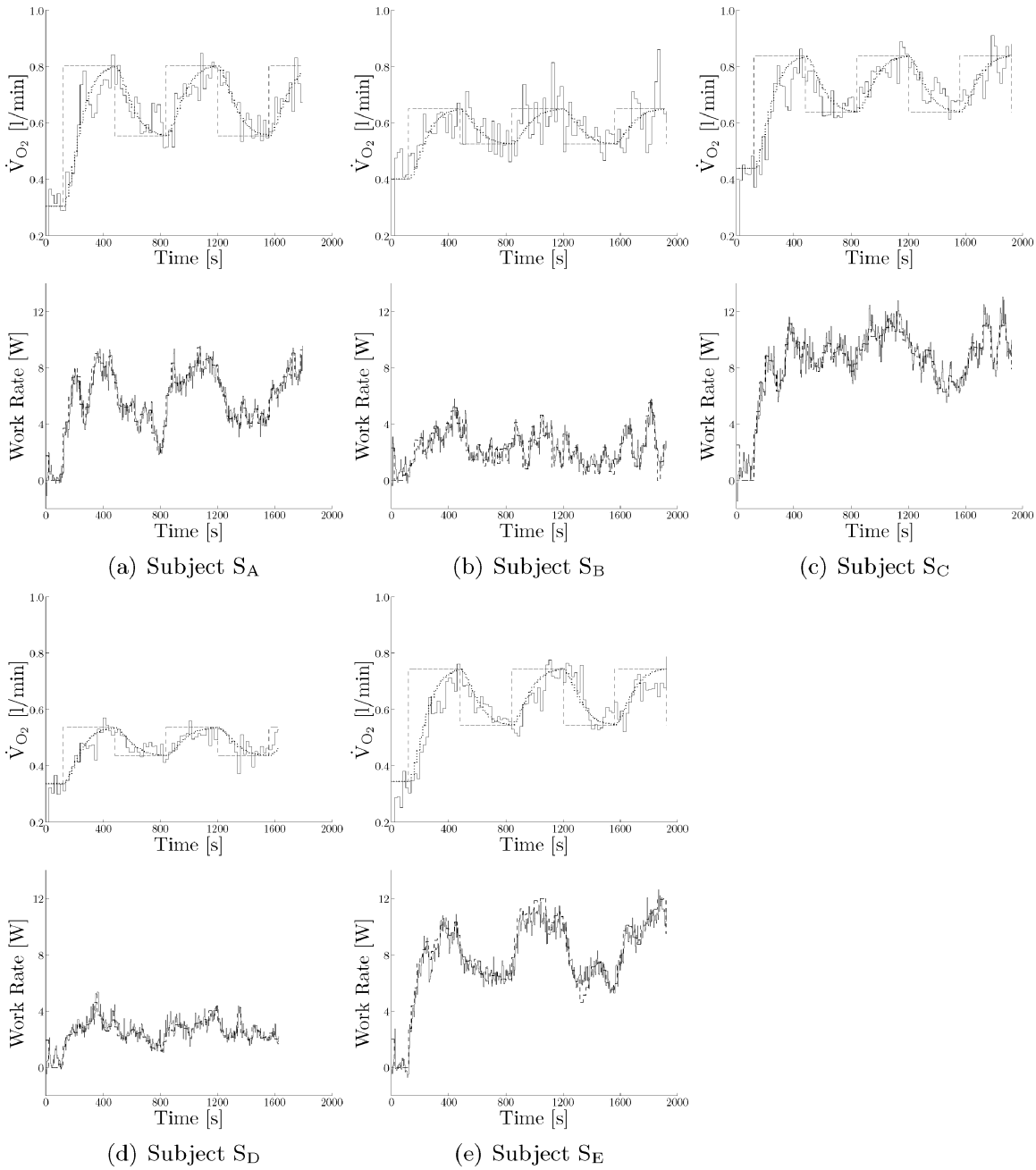

Fig. 7. Experimental control test results. For each subject, the oxygen-uptake-rate ($\dot{V}_{O_2}$) results are shown along with the work-rate data. In the upper plot for each subject, the reference $\dot{V}_{O_2}$ is drawn as a dashed line, the ideal response as specified by pole placement as a dotted line, and the actual recorded $\dot{V}_{O_2}$ measurement as a solid line. In the lower plot for each subject, the averaged work-rate measurement is shown as a solid line while the reference work rate is depicted as a dashed line. Note that, for clarity of display, the recorded work-rate data have been averaged over 4-s periods.

lines in the upper plot of each subfigure. The ideal responses are those as specified in the pole-placement routine in terms of rise time and damping factor. Under each $\dot{V}_{O_2}$ result, the corresponding mechanical work rate for each test is plotted. The measured work rate is shown as a solid line while the reference work rate is depicted as a dashed line in each case.

The plots show that the exercisers successfully produced their required work rates and, furthermore, that the $\dot{V}_{O_2}$ step responses for all subjects tend toward the reference values, closely following the ideal $\dot{V}_{O_2}$ signals.

IV. Discussion

We aimed to devise a control system which would automatically regulate the level of oxygen uptake to desired levels during rBWSTT ambulation. The proposed approach to real-time $\dot{V}_{O_2}$ control was demonstrated to be feasible, with the resulting closed-loop structure showing an adequate robustness of stability and performance properties. A stable response was elicited from each subject using the same control polynomials; moreover, the $\dot{V}_{O_2}$ output signal, although noisy, tends toward

the desired reference values and follows the ideal response in each case.

It is clear that the robustness characteristics of the resulting closed-loop system are important due to the uncertainty in the model of the underlying dynamics. The fit achieved during the identification process was relatively low, indicating a high degree of uncertainty in the model. The stability margin of the nominal system suggests that the closed-loop structure is nominally stable with a satisfactory vector margin. Although the control polynomials were based on the dynamics of subject S_A, the quality of reference tracking is not discernibly different across subjects, indicating a satisfactory robustness of performance of the proposed system.

The work-rate reference signals respond in such a way as to give the desired $\dot{V}_{O_2}$ output. However, they are sensitive to the noise corruption $n(t)$. In principle, this sensitivity can be reduced by incorporating a prefilter adjacent to the input $r(t)$[13], [19]. The polynomial for the response from $r(t)$ to $y(t)$ can be set as desired and decoupled from the responses to the other variables, while the polynomials governing the responses to the disturbance $d(t)$ and noise $n(t)$ can be adjusted and reduced in bandwidth in order to lower the sensitivity of the control signal $u(t)$ to the noise and thereby smooth its response.

A comparison of the steady-state work rates and corresponding $\dot{V}_{O_2}$ responses shows that the exercise performed appears to be much less efficient than regular able-bodied exercise. This low computed efficiency results from an underestimation of the total work done—the calculation neglects work done against gravity and also that produced by the shear forces at the feet on the treadmill itself [20]. The estimation method aims at reflecting the intensity of the exercise in a quantitative manner without necessarily being a true measure of the actual total mechanical work done [14].

The proposed control concept and structure are therefore feasible for real-time control of oxygen uptake during robot-assisted gait, as verified in tests with able-bodied subjects. The control of $\dot{V}_{O_2}$ with neurologically impaired subjects gives rise to additional challenges due to their decreased capacity for control and range of work rates that may be produced. Moreover, as a result of their altered autonomic nervous-system physiology, subjects with a spinal-cord injury often produce complex $\dot{V}_{O_2}$ responses that may be difficult to model. Further work is therefore merited to investigate the applicability of this approach in neurologically impaired subjects.

V. Conclusion

The proposed feedback structure for $\dot{V}_{O_2}$ control during robot-assisted gait training with able-bodied subjects was demonstrated to be feasible, with the system showing satisfactory reference input tracking behavior and robustness of stability and performance characteristics. This moves toward the use of robotic body-weight-supported treadmill technology in practical exercise training and testing programs.

Further work is required to test the concept with neurologically impaired subjects, a task which will pose additional modeling and control challenges.

References

[1] J. Galvez and D. Reinkensmeyer, "Robotics for gait training after spinal cord injury," *Top. Spinal Cord Inj. Rehabil.*, vol. 11, no. 2, pp. 18–33, 2005.

[2] T. G. Hornby, D. Campbell, D. Zemon, and J. Kahn, "Clinical and quantitative evaluation of robotic-assisted treadmill walking to retrain ambulation after spinal cord injury," *Top. Spinal Cord Inj. Rehabil.*, vol. 11, no. 2, pp. 1–17, 2005.

[3] M. Wirz, D. Zemon, R. Rupp, A. Scheel, G. Colombo, V. Dietz, and G. Hornby, "Effectiveness of automated locomotor training in patients with chronic incomplete spinal cord injury: A multicenter trial," *Arch. Phys. Med. Rehabil.*, vol. 86, no. 4, pp. 672–680, Apr. 2005.

[4] J. F. Israel, D. D. Campbell, J. H. Kahn, and T. G. Hornby, "Metabolic costs and muscle activity patterns during robotic- and therapist-assisted treadmill walking in individuals with incomplete spinal cord injury," *Phys. Ther.*, vol. 86, no. 11, pp. 1466–1478, Nov. 2006.

[5] C. Krewer, F. Müller, B. Husemann, S. Heller, J. Quintern, and E. Koenig, "The influence of different Lokomat walking conditions on the energy expenditure of hemiparetic patients and healthy subjects," *Gait Posture*, vol. 26, no. 3, pp. 372–377, Sep. 2006.

[6] M. Nash, P. Jacobs, B. Johnson, and E. Field-Fote, "Metabolic and cardiac responses to robotic-assisted locomotion in motor-complete tetraplegia: A case report," *J. Spinal Cord Med.*, vol. 27, no. 1, pp. 78–82, 2004.

[7] R. L. Johnson, K. A. Gerhart, J. McCray, J. C. Menconi, and G. G. Whiteneck, "Secondary conditions following spinal cord injury in a population-based sample," *Spinal Cord*, vol. 36, no. 1, pp. 45–50, Jan. 1998.

[8] T. Janssen, A. Dallmeijer, D. Veeger, and L. van der Woude, "Normative values and determinants of physical capacity in individuals with spinal cord injury," *J. Rehabil. Res. Dev.*, vol. 39, no. 1, pp. 29–39, Jan./Feb. 2002.

[9] S. Muraki, N. Tsunawake, Y. Tahara, S. Hiramatsu, and M. Yamasaki, "Multivariate analysis of factors influencing physical work capacity in wheelchair-dependent paraplegics with spinal cord injury," *Med. Sci. Sports Exerc.*, vol. 81, no. 1/2, pp. 28–32, Jan. 2000.

[10] L. Lünenburger, G. Colombo, and R. Riener, "Biofeedback for robotic gait rehabilitation," *J. NeuroEng. Rehabil.*, vol. 4, no. 1, pp. 1–11, Jan. 2007.

[11] L. Lünenburger, G. Colombo, R. Riener, and V. Dietz, "Biofeedback in gait training with the robotic orthosis Lokomat," in *Proc. 26th Annu. Conf. IEEE EMBS*, San Francisco, CA, 2004, pp. 4888–4891.

[12] K. J. Hunt, L. P. Jack, A. Pennycott, C. Perret, M. Baumberger, and T. H. Kakebeeke, "Control of work rate-driven exercise facilitates cardiopulmonary training and assessment during robot-assisted gait in incomplete spinal cord injury," *Biomed. Signal Process. Control*, vol. 3, no. 1, pp. 19–28, Jan. 2008.

[13] K. J. Hunt, O. Ajayi, H. Gollee, and L. Jamieson, "Feedback control of oxygen uptake during treadmill exercise," *IEEE Trans. Control Syst. Technol.*, vol. 16, no. 4, pp. 624–635, Jul. 2008.

[14] A. Pennycott, K. J. Hunt, L. P. Jack, C. Perret, and T. H. Kakebeeke, "Estimation and volitional feedback control of active work during robotic-assisted gait," *Control Eng. Pract.*, vol. 17, no. 2, pp. 322–328, Feb. 2009.

[15] W. McArdle, F. Katch, and V. Katch, *Essentials of Exercise Physiology*, 3rd ed. Philadelphia, PA : Lippincott Williams & Wilkins, 2001.

[16] M. Pollock, G. Gaesser, J. Butcher, J. Despres, R. Dishman, B. Franklin, and C. Garber, "The recommended quantity and quality of exercise for developing and maintaining cardiorespiratory and muscular fitness, and flexibility in healthy adults," *Med. Sci. Sports Exerc.*, vol. 30, no. 6, pp. 975–991, Jun. 1998.

[17] K. J. Hunt, B. Stone, and D. B. Allan, "Feedback control of oxygen uptake during stimulated cycle ergometry in paraplegic subjects," *IET Control Theory Appl.*, vol. 2, no. 6, pp. 488–495, Jun. 2008.

[18] M. Frey, G. Colombo, M. Vaglio, R. Bucher, M. Jörg, and R. Riener, "A novel mechatronic body weight support system," *IEEE Trans. Neural Syst. Rehabil. Eng.*, vol. 14, no. 3, pp. 311–321, Sep. 2006.

[19] K. J. Åström and B. Wittenmark, *Computer-Controlled Systems: Theory for the User*, 2nd ed. Englewood Cliffs, NJ: Prentice-Hall, 1990.

[20] A. Pennycott, "The application of estimation and control techniques in two modes of exercise for the spinal cord injured," Ph.D. dissertation, Univ. Glasgow, Glasgow, Scotland, 2008.

[21] L. Ljung, *System Identification: Theory for the User*. Englewood Cliffs, NJ: Prentice-Hall, 1987.